

Analysis of the rare semileptonic decays of B_s to $f_0(980)$ and $K_0^*(1430)$ scalar mesons in QCD sum rules

N. Ghahramany* and R. Khosravi†

Physics Department, Shiraz University, Shiraz 71454, Iran
(Received 27 April 2009; published 29 July 2009)

We investigate the rare semileptonic decays $B_s \rightarrow [f_0(980), K_0^*(1430)]l^+l^-$, ($l = e, \mu, \tau$), and $B_s \rightarrow [f_0(980), K_0^*(1430)]\nu\bar{\nu}$ in the framework of the three-point QCD sum rules. These decays are important to study because the $f_0(980)$ and $K_0^*(1430)$ are the scalar mesons with total spin 0 and even parity and the quark content of them are still controversial in high energy physics. These rare decays occur at loop level by electroweak penguin and weak box diagrams in the standard model via the flavor changing neutral current transitions of $b \rightarrow d, s$, and not allowed by tree level. Considering the effective contributions of the nonperturbative parts of the correlation function, we calculate the relevant form factors of these transitions. The branching fractions and longitudinal lepton polarization asymmetry are also investigated.

DOI: 10.1103/PhysRevD.80.016009

PACS numbers: 11.55.Hx, 13.20.He

I. INTRODUCTION

The scalar mesons with total spin 0 and even parity are often produced in proton-antiproton annihilation, decays of heavy flavor mesons, meson scattering, and ϕ radiative decays. The light scalar mesons are important to study because their quark content is still a common problem for high energy physics and may be interpreted in a number of different ways, for example, considering as a tetra quark multiplet [1–3], or as a meson-meson molecules state [4–8]. The light scalar mesons which have been observed by experiment, with regard to their isospin value, are classified as follows [9]:

- (1) $\kappa(800)$ and $K_0^*(1430)$ with isospin $I = 1/2$,
- (2) $\sigma(600)$, $f_0(980)$, $f_0(1370)$, $f_0(1500)$, and $f_0(1710)$ with isospin $I = 0$,
- (3) $a_0(980)$, $a_0(1450)$ with isospin $I = 1$.

It is most possible that all of the above mesons make up a flavor nonet [9,10]. We would like to consider the $f_0(980)$ and $K_0^*(1430)$ light scalar mesons via the semileptonic $B_s \rightarrow [f_0(980), K_0^*(1430)]$ transitions.

The flavor structure of the $f_0(980)$ meson has not been known outright. It has been interpreted as a $s\bar{s}$ state [11–13], as a four quark $s\bar{s}q\bar{q}$ state [1], and as a bound state of hadrons [4,14]. The recently measured relative weight of the $D_s^+ \rightarrow f_0(980)\pi^+ \rightarrow \pi^+\pi^-\pi^+$ decay [15] may serve as a tool for the estimation of the $s\bar{s}$ component of the $f_0(980)$ meson. But the observation $\Gamma(j/\psi \rightarrow f_0(980)\omega) \simeq \Gamma(j/\psi \rightarrow f_0(980)\phi)$ indicates that the quark content of $f_0(980)$ is not purely the $s\bar{s}$ state, but should have non-strange parts, too [16]. Therefore in the quark model, $f_0(980)$ should be a mixture of $s\bar{s}$ and $u\bar{u} + d\bar{d}$ as [17]

$$|f_0(980)\rangle = \cos\theta|s\bar{s}\rangle + \frac{\sin\theta}{\sqrt{2}}|u\bar{u} + d\bar{d}\rangle. \quad (1)$$

In Ref. [16], analysis of the experimental data shows that the mixing angle θ lies in the ranges $25^\circ < \theta < 40^\circ$ and $140^\circ < \theta < 165^\circ$. The mixing angle $35^\circ < \theta < 55^\circ$ was found in Ref. [18].

The $K_0^*(1430)$ is perhaps the least controversial of the light scalar meson. Almost every model of scalar states agree that $K_0^*(1430)$ is dominated by the $s\bar{u}$ or $s\bar{d}$ state. The predicted mass and bound state of the $K_0^*(1430)$ meson from QCD sum rules approach is consistent with the $s\bar{u}$ or $s\bar{d}$ state, too [19].

The rare semileptonic $B_s \rightarrow [f_0(980), K_0^*(1430)] \times l^+l^-/\nu\bar{\nu}$ decays occur at loop level by electroweak penguin and weak box diagrams in the standard model (SM) via the flavor changing neutral current (FCNC) transitions of $b \rightarrow d, s$. Therefore the future experimental study of such rare decays can improve the information about:

- (i) precise values for the Cabibbo, Kobayashi, Maskawa (CKM) matrix elements in the weak interactions,
- (ii) CP violation, T violation and polarization asymmetries in $b \rightarrow d, s$ penguin channels,
- (iii) new operators or operators that are subdominant in the SM,
- (iv) establishing new physics (NP) and flavor physics beyond the SM.

The FCNC decays of the B meson are sensitive to NP contributions to penguin operators. So to test the SM and look for NP, we need to determine the SM predictions for FCNC decays and compare these results to the corresponding experimental values.

The QCD sum rules have been successfully applied to a wide variety of problems in hadron physics. So far the semileptonic decays of B involving $K(K^*, K_0^*)$ such as $B \rightarrow Kl^+l^-$, $B \rightarrow K^*l^+l^-$ [20], and $B_s \rightarrow K_0^*(1430)l\nu$ [10] have been studied in the framework of the three-point QCD sum rules. Also, considering $SU_f(3)$ symmetry and ignoring the mass of u and d , the semileptonic $B \rightarrow K_0^*(1430)l^+l^-$ decay has been analyzed in this manner, before [21]. But in this paper, the semileptonic $B_s \rightarrow [f_0(980), K_0^*(1430)]l^+l^-$

*ghahramany@susc.ac.ir
†khosravi.reza@gmail.com

decays are investigated via $SU_f(3)$ symmetry breaking. For the stated purpose, the mass of the spectator s quark has been considered in the expressions of the quark condensates and spectral densities, therefore the spectral densities and nonperturbative part contributions (in our case, quark condensate) are different from those in Ref. [21].

For analysis of the above mentioned decays, using the operator product expansion (OPE) in the deep Euclidean region and considering the contributions of the operators with dimension 3, 4, and 5, we calculate the transition form factors of the semileptonic $B_s \rightarrow [f_0(980), K_0^*(1430)]$ decays. Also, we consider the branching ratio values and longitudinal lepton polarization asymmetry of these semileptonic decays. Note that, to analyze the $B_s \rightarrow f_0(980)$ transition, we consider only the $|s\bar{s}\rangle$ state part of Eq. (1) for the $f_0(980)$ meson.

This paper is organized as follows: The three-point QCD sum rules approach for calculation of the relevant form factors are presented in Sec. II. The contributions of the nonperturbative part of the correlation function, calculations of them, and the decay rate formulas for $B_s \rightarrow [f_0(980), K_0^*(1430)]l^+l^-$ and $B_s \rightarrow [f_0(980), K_0^*(1430)]\nu\bar{\nu}$ decays are presented in Sec. III. The next section is devoted to numeric results and discussions. In this part, we report the branching ratio values of the considered decays. For a better analysis, we plot the transition form factors and longitudinal lepton polarization asymmetry related to these semileptonic decays with respect to the momentum transfer squared q^2 .

II. THE QCD SUM RULES METHOD

At quark level, $b \rightarrow q'l^+l^-$, ($q' = d, s$) transitions take place via electromagnetic and Z penguin and W box diagrams in the SM and are not allowed in the tree level. These loop transitions occur via the intermediate u, c, t quarks. In the SM, the measurement of the forward-backward asymmetry and invariant dilepton mass distribution in $b \rightarrow q'l^+l^-$ transitions provide information on the short distance contributions dominated by the top quark loops [22].

The rare semileptonic $B_s \rightarrow Sl^+l^-$, ($l = e, \mu, \tau$) and $B_s \rightarrow S\nu\bar{\nu}$ decays, where S stands for the $f_0(980)$ or $K_0^*(1430)$ scalar meson, occur by the loop $b \rightarrow q'\bar{l}l$ transitions. The electroweak penguin involving the contributions of photon and Z boson is shown in Fig. 1. It is reminded that the $b \rightarrow q'\nu\bar{\nu}$ transitions receive contributions only from Z penguin and box diagrams. The effective Hamiltonian responsible for these decays is described in terms of the Wilson coefficients, C_7^{eff} , C_9^{eff} , and C_{10} as

$$\begin{aligned} \mathcal{H}_{\text{eff}} = & \frac{G_F \alpha}{2\sqrt{2}\pi} V_{ib} V_{iq'}^* \left[C_9^{\text{eff}} \bar{q}' \gamma_\mu (1 - \gamma_5) b \bar{\ell} \gamma_\mu \ell \right. \\ & + C_{10} \bar{q}' \gamma_\mu (1 - \gamma_5) b \bar{\ell} \gamma_\mu \gamma_5 \ell \\ & \left. - 2C_7^{\text{eff}} \frac{m_b}{q^2} \bar{q}' i \sigma_{\mu\nu} q^\nu (1 + \gamma_5) b \bar{\ell} \gamma_\mu \ell \right], \quad (2) \end{aligned}$$

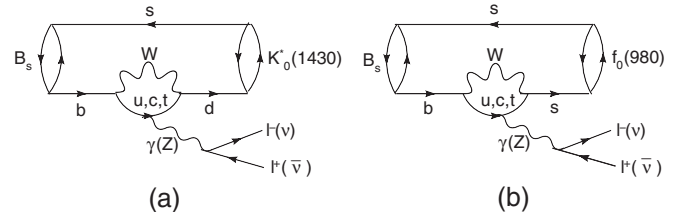


FIG. 1. Semileptonic decays of B_s involving $K_0^*(1430)$ or $f_0(980)$. Penguin diagram (a) for $B_s \rightarrow K_0^*(1430)l^+l^-/\nu\bar{\nu}$ and penguin diagram (b) for $B_s \rightarrow f_0(980)l^+l^-/\nu\bar{\nu}$.

where G_F is the Fermi constant, α is the fine structure constant at Z mass scale, and V_{ij} are elements of the CKM matrix. For the $\nu\bar{\nu}$ case, only the term containing C_{10} is considered. The matrix elements of $B_s \rightarrow Sl^+l^-/\nu\bar{\nu}$ decays are calculated by inserting Eq. (2) between the initial and final meson states:

$$\begin{aligned} \mathcal{M} = & \frac{G_F \alpha}{2\sqrt{2}\pi} V_{ib} V_{iq'}^* \left[C_9^{\text{eff}} \langle S(p') | \bar{q}' \gamma_\mu (1 - \gamma_5) b | B_s(p) \rangle \right. \\ & \times \bar{\ell} \gamma_\mu \ell + C_{10} \langle S(p') | \bar{q}' \gamma_\mu (1 - \gamma_5) b | B_s(p) \rangle \\ & \times \bar{\ell} \gamma_\mu \gamma_5 \ell - 2C_7^{\text{eff}} \frac{m_b}{q^2} \\ & \left. \times \langle S(p') | \bar{q}' i \sigma_{\mu\nu} q^\nu (1 + \gamma_5) b | B_s(p) \rangle \bar{\ell} \gamma_\mu \ell \right]. \quad (3) \end{aligned}$$

We consider the hadronic matrix elements $\langle S(p') | \bar{q}' \gamma_\mu (1 - \gamma_5) b | B_s(p) \rangle$ and $\langle S(p') | \bar{q}' i \sigma_{\mu\nu} q^\nu (1 + \gamma_5) b | B_s(p) \rangle$ appearing in the above equation. Because of the parity conservation, the vector current does not contribute to the pseudoscalar-scalar hadronic matrix element, i.e.,

$$\langle S(p') | \bar{q}' \gamma_\mu b | B_s(p) \rangle = 0, \quad \langle S(p') | \bar{q}' i \sigma_{\mu\nu} q^\nu b | B_s(p) \rangle = 0. \quad (4)$$

From Lorentz invariance, these matrix elements can be parametrized in terms of form factors in the following way:

$$\langle S(p') | \bar{q}' \gamma_\mu \gamma_5 b | B_s(p) \rangle = -i(\mathcal{P}_\mu f_+(q^2) + q_\mu f_-(q^2)), \quad (5)$$

$$\begin{aligned} \langle S(p') | \bar{q}' i \sigma_{\mu\nu} q^\nu \gamma_5 b | B_s(p) \rangle = & \frac{f_T(q^2)}{m_{B_s} + m_S} [\mathcal{P}_\mu q^2 \\ & - q_\mu (m_{B_s}^2 - m_S^2)], \quad (6) \end{aligned}$$

where $f_+(q^2)$, $f_-(q^2)$, and $f_T(q^2)$ are the transition form factors, which only depend on the momentum transfer squared q^2 , $\mathcal{P}_\mu = (p + p')_\mu$, and $q_\mu = (p - p')_\mu$. Here, we should mention that for the $\nu\bar{\nu}$ case, the form factor $f_T(q^2)$ does not contribute since it is related to the photon vertex ($\sigma_{\mu\nu} q^\nu \gamma_5$).

To calculate the form factors $f_+(q^2)$, $f_-(q^2)$, and $f_T(q^2)$, in the three-point QCD sum rules, we start with the correlation function. The three correlation function can

be constructed from the vacuum expectation value of the time ordered product of interpolating fields and axial transition currents J^A and J^T , as follows:

$$\Pi_{\mu}^{A,T} = i^2 \int d^4x d^4y e^{-ipx} e^{ip'y} \langle 0 | \mathcal{T} \{ J_S(y) J_{\mu}^{A,T}(0) J_{B_s}^{\dagger}(x) \} | 0 \rangle, \quad (7)$$

where $J_{B_s}(x) = \bar{s}\gamma_5 b$, $J_S(y) = \bar{s}q'$. $J_{B_s}(x)$ and $J_S(y)$ are the interpolating currents of the S and B_s mesons and $J_{\mu}^A = \bar{q}'\gamma_{\mu}\gamma_5 b$ and $J_{\mu}^T = \bar{q}'\sigma_{\mu\nu}q'\gamma_5 b$ are the axial transition currents. For extracting the expressions for form factors $f_+(q^2)$ and $f_-(q^2)$, we choose the coefficients of the

structures \mathcal{P}_{μ} and q_{μ} from $\Pi_{\mu}^A(p^2, p'^2, q^2)$, respectively, and the structure q_{μ} from $\Pi_{\mu}^T(p^2, p'^2, q^2)$ is considered for the form factor $f_T(q^2)$. Therefore, the correlation functions are written in terms of the selected structures as

$$\begin{aligned} \Pi_{\mu}^A(p^2, p'^2, q^2) &= \Pi_+ \mathcal{P}_{\mu} + \Pi_- q_{\mu}, \\ \Pi_{\mu}^T(p^2, p'^2, q^2) &= \Pi_T q_{\mu} + \dots \end{aligned} \quad (8)$$

The phenomenological part of the correlation function can be obtained by inserting the complete set of intermediate states with the same quantum numbers as the currents J_S and J_{B_s} . As a result of this procedure

$$\Pi_{\mu}^{A,T}(p^2, p'^2, q^2) = \frac{\langle 0 | J_S | S(p') \rangle \langle S(p') | J_{\mu}^{A,T} | B_s(p) \rangle \langle B_s(p) | J_{B_s}^{\dagger} | 0 \rangle}{(m_S^2 - p'^2)(m_{B_s}^2 - p^2)} + \text{higher resonances and continuum states} \quad (9)$$

is obtained. The following matrix elements are defined in terms of the leptonic decay constants of the S and B_s mesons as

$$\langle 0 | J_S | S \rangle = f_S m_S, \quad \langle 0 | J_{B_s} | B_s \rangle = -i \frac{f_{B_s} m_{B_s}^2}{m_b + m_s}. \quad (10)$$

Using Eqs. (5), (6), and (10) in Eq. (9), we obtain

$$\begin{aligned} \Pi_{\mu}^A(p^2, p'^2, q^2) &= \frac{f_{B_s} m_{B_s}^2}{(m_b + m_s)} \frac{f_S m_S}{(m_S^2 - p'^2)(m_{B_s}^2 - p^2)} [f_+(q^2) \mathcal{P}_{\mu} + f_-(q^2) q_{\mu}], \\ \Pi_{\mu}^T(p^2, p'^2, q^2) &= \frac{f_{B_s} m_{B_s}^2}{(m_b + m_s)} \frac{f_S m_S}{(m_S^2 - p'^2)(m_{B_s}^2 - p^2)} \left[\frac{f_T(q^2)}{(m_{B_s} + m_S)} (q^2 \mathcal{P}_{\mu} - (m_{B_s}^2 - m_S^2) q_{\mu}) \right]. \end{aligned} \quad (11)$$

Now, we would like to calculate the QCD part of the correlation functions. For this aim, we write each Π_i function in terms of the perturbative and nonperturbative parts as

$$\Pi_i(p^2, p'^2, q^2) = \Pi_i^{\text{per}}(p^2, p'^2, q^2) + \Pi_i^{\text{nonper}}(p^2, p'^2, q^2), \quad (12)$$

where i stands for $+$, $-$, and T . For the perturbative part, the bare loop diagrams (Fig. 1) are considered. In calculating the bare loop contribution, we first write the double dispersion representation for the coefficients of the corresponding Lorentz structures appearing in each correlation function, as

$$\begin{aligned} \Pi_i^{\text{per}} &= -\frac{1}{(2\pi)^2} \int ds' \int ds \frac{\rho_i^{\text{per}}(s, s', q^2)}{(s - p^2)(s' - p'^2)} \\ &+ \text{subtraction terms.} \end{aligned} \quad (13)$$

The spectral densities $\rho_i^{\text{per}}(s, s', q^2)$ are calculated by the help of the Cutkosky rules, i.e., the propagators are replaced by Dirac-delta functions

$$\frac{1}{p^2 - m^2} \rightarrow -2i\pi\delta(p^2 - m^2), \quad (14)$$

expressing that all quarks are real. The integration region in Eq. (13) is obtained by requiring that the argument of three delta vanish, simultaneously. The physical region in the s and s' plane is described by the following inequalities:

$$\begin{aligned} -1 &\leq \frac{2ss' + (s + s' - q^2)(m_b^2 - m_s^2 - s) + 2s(m_s^2 - m_{q'}^2)}{\lambda^{1/2}(s, s', q^2)\lambda^{1/2}(m_b^2, m_s^2, s)} \\ &\leq +1, \end{aligned} \quad (15)$$

where $\lambda(a, b, c) = a^2 + b^2 + c^2 - 2ab - 2ac - 2bc$. From this inequality, to use in the lower limit of the integration over s in Eq. (13), it is easy to express s in terms of s' , i.e., s_L is as follows:

$$s_L = \frac{(m_s^2 + q^2 - m_b^2 - s')(m_b^2 s' - q^2 m_s^2)}{(m_b^2 - q^2)(m_s^2 - s')}. \quad (16)$$

Straightforward calculations end up in the following results for the spectral densities:

$$\begin{aligned}
 \rho_+^A(s, s', q^2) &= -I_0 N_c \{ \Delta + \Delta' - 2m_s [(2 + E_1 + E_2)m_s + (1 + E_1 + E_2)m_{q'}] \\
 &\quad + 2m_b [(1 + E_1 + E_2)m_s + (E_1 + E_2)m_{q'}] + (E_1 + E_2)u \}, \\
 \rho_-^A(s, s', q^2) &= I_0 N_c \{ \Delta - \Delta' + 2m_s [(E_1 - E_2 + 1)m_{q'} + (E_1 - E_2)m_s] \\
 &\quad - 2m_b [(E_1 - E_2 - 1)m_s + (E_1 - E_2)m_{q'}] + (E_2 - E_1)u \}, \\
 \rho_T^T(s, s', q^2) &= I_0 N_c \{ \Delta(m_b - 2m_s - m_{q'}) + \Delta'(2m_s - m_b + m_{q'}) + 2[m_s(E_2 - E_1 + 1) + m_{q'}(E_2 - E_1)]s \\
 &\quad + 2[m_b(E_1 - E_2) + m_s(E_2 - E_1 - 1)]s' + (E_1 - E_2)(2m_s - m_b + m_{q'})u \},
 \end{aligned} \tag{17}$$

where

$$\begin{aligned}
 I_0(s, s', q^2) &= \frac{1}{4\lambda^{1/2}(s, s', q^2)}, \quad \lambda(s, s', q^2) = s^2 + s'^2 + q^4 - 2sq^2 - 2s'q^2 - 2ss', \quad E_1 = \frac{1}{\lambda(s, s', q^2)} [2s'\Delta - \Delta'u], \\
 E_2 &= \frac{1}{\lambda(s, s', q^2)} [2s\Delta' - \Delta u], \quad u = s + s' - q^2, \quad \Delta = s + m_s^2 - m_b^2, \quad \Delta' = s' + m_s^2 - m_{q'}^2,
 \end{aligned} \tag{18}$$

and $N_c = 3$ is the color factor.

III. CONDENSATE TERM CONTRIBUTIONS

In this section, the nonperturbative part contributions to the correlation function are discussed [Eq. (12)]. In QCD, the three-point correlation function can be evaluated by the OPE in the deep Euclidean region where $p^2 \ll (m_b + m_s)^2$, $p'^2 \ll (m_s^2 + m_{q'}^2)$. For this aim, we expand the time ordered products of currents contained in the three-point correlation function in terms of a series of local operators with increasing dimension results in the following form [10]:

$$\begin{aligned}
 & - \int d^4x d^4y e^{i(px - p'y)} T \{ J_S J_\mu^A J_{B_s}^\dagger \} \\
 &= (C_0)_\mu I + (C_3)_\mu \bar{\Psi} \Psi + (C_4)_\mu G_{\alpha\beta}^a G^{a\alpha\beta} \\
 &\quad + (C_5)_\mu \bar{\Psi} \sigma_{\alpha\beta} T^a G^{a\alpha\beta} \Psi + (C_6)_\mu \bar{\Psi} \Gamma \Psi \bar{\Psi} \Gamma' \Psi \\
 &\quad + \dots,
 \end{aligned} \tag{19}$$

where $(C_i)_\mu$ are the Wilson coefficients, $G_{\alpha\beta}$ is the gluon field strength tensor, I is the unit operator, Ψ is the local fermion field operator of quarks, and Γ and Γ' are the matrices appearing in the calculations. Taking into account the vacuum expectation value of the OPE, the expansion of the correlation function in terms of local operators is written as follows:

$$\begin{aligned}
 \Pi_\mu(p^2, p'^2, q^2) &= C_{0\mu} + C_{3\mu} \langle \bar{\Psi} \Psi \rangle + C_{4\mu} \langle G^2 \rangle \\
 &\quad + C_{5\mu} \langle \bar{\Psi} \sigma_{\alpha\beta} T^a G^{a\alpha\beta} \Psi \rangle \\
 &\quad + C_{6\mu} \langle \bar{\Psi} \Gamma \Psi \bar{\Psi} \Gamma' \Psi \rangle + \dots
 \end{aligned} \tag{20}$$

In Eq. (20), the first term is related to the contribution of the perturbative part of correlation function and the rest terms are related to the nonperturbative contributions of it. The contribution of the perturbative part was discussed before. Now we consider the condensate terms of dimension 3, 4, and 5. The condensate terms of dimensions 3 and

5 are related to contributions of quark condensate and quark-gluon condensate, respectively. It is found that the heavy quark condensate contributions are exponentially suppressed by heavy quark masses and can be safely omitted. The light q' quark condensate contribution is zero after applying the double Borel transformation with respect to both variables p^2 and p'^2 , because only one variable appears in the denominator. Our calculations show that in this case, the gluon condensate contributions are very small in comparison with the quark condensate contributions and we can easily ignore their contributions in our calculations. Therefore only six important diagrams remain from the nonperturbative part contributions. The diagrams of the effective contributions of the condensate terms are depicted in Fig. 2.

In our calculation, the following Borel transformations are also used:

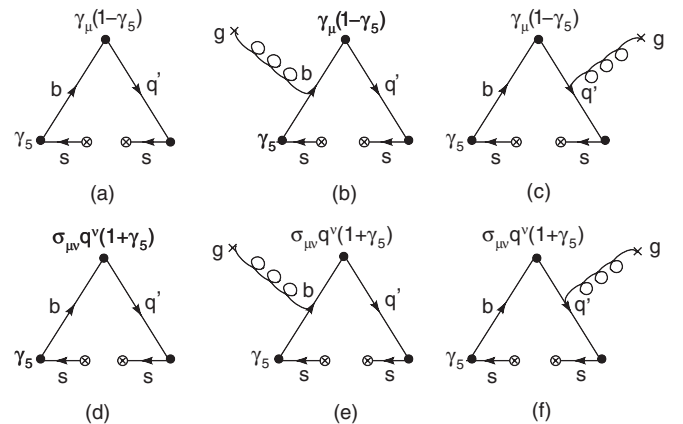


FIG. 2. The diagrams of the effective contributions of the condensate terms.

$$\begin{aligned}\mathcal{B}_{p^2}(M_1^2)\left(\frac{1}{p^2 - m_b^2}\right)^m &= \frac{(-1)^m e^{-(m_b^2/M_1^2)}}{\Gamma(m) (M_1^2)^m}, \\ \mathcal{B}_{p'^2}(M_2^2)\left(\frac{1}{p'^2 - m_q^2}\right)^n &= \frac{(-1)^n e^{-(m_q^2/M_2^2)}}{\Gamma(n) (M_2^2)^n}.\end{aligned}\quad (21)$$

The next step is to apply the Borel transformations with respect to the $p^2(p^2 \rightarrow M_1^2)$ and $p'^2(p'^2 \rightarrow M_2^2)$ on the phenomenological as well as the perturbative and non-perturbative parts of the correlation functions and equate these two representations of the correlations. The following sum rules for the form factors $f_+(q^2)$, $f_-(q^2)$, and $f_T(q^2)$ are derived:

$$\begin{aligned}f_+(q^2) &= \frac{(m_b + m_s)}{f_{B_s} m_{B_s}^2 f_S m_S} e^{m_{B_s}^2/M_1^2} e^{m_S^2/M_2^2} \left\{ -\frac{1}{4\pi^2} \int_{(m_s+m_q)^2}^{s'_0} ds' \right. \\ &\quad \times \int_{s_L}^{s_0} ds \rho_+^A(s, s', q^2) e^{-s/M_1^2} e^{-s'/M_2^2} \\ &\quad \left. + \tilde{B} \Pi_+^{\text{nonper}}(p^2, p'^2, q^2) \right\},\end{aligned}\quad (22)$$

$$\begin{aligned}f_-(q^2) &= \frac{(m_b + m_s)}{f_{B_s} m_{B_s}^2 f_S m_S} e^{m_{B_s}^2/M_1^2} e^{m_S^2/M_2^2} \left\{ -\frac{1}{4\pi^2} \int_{(m_s+m_q)^2}^{s'_0} ds' \right. \\ &\quad \times \int_{s_L}^{s_0} ds \rho_-^A(s, s', q^2) e^{-s/M_1^2} e^{-s'/M_2^2} \\ &\quad \left. + \tilde{B} \Pi_-^{\text{nonper}}(p^2, p'^2, q^2) \right\},\end{aligned}\quad (23)$$

$$\begin{aligned}f_T(q^2) &= \frac{(m_b + m_s)}{f_{B_s} m_{B_s}^2 f_S m_S (m_{B_s} - m_S)} e^{m_{B_s}^2/M_1^2} e^{m_S^2/M_2^2} \\ &\quad \times \left\{ -\frac{1}{4\pi^2} \int_{(m_s+m_q)^2}^{s'_0} ds' \int_{s_L}^{s_0} ds \rho_T^T(s, s', q^2) e^{-s/M_1^2} \right. \\ &\quad \left. \times e^{-s'/M_2^2} + \tilde{B} \Pi_T^{\text{nonper}}(p^2, p'^2, q^2) \right\},\end{aligned}\quad (24)$$

where s_0 and s'_0 are the continuum thresholds and s_L is the lower limit of the integral over s presented in Eq. (16). Also \tilde{B} is

$$\tilde{B} = \mathcal{B}_{p^2}(M_1^2) \mathcal{B}_{p'^2}(M_2^2).\quad (25)$$

The explicit expressions of the $\Pi_i^{\text{nonper}}(p^2, p'^2, q^2)$, $i = +, -, T$ of the quark condensate coefficients with dimensions 3 and 5 are given in the Appendix.

In the above equations, in order to subtract the contributions of the higher states and the continuum, the quark-hadron duality assumption is also used, i.e., it is assumed that

$$\rho^{\text{higher states}}(s, s') = \rho^{\text{OPE}}(s, s') \theta(s - s_0) \theta(s' - s'_0).\quad (26)$$

At the end of this section, we would like to present the differential decay widths of the $B_s \rightarrow Sl^+l^-$ and $B_s \rightarrow S\nu\bar{\nu}$ decays. Using the parametrization of these transitions

in terms of the form factors and amplitude in Eq. (3), we get [23]

$$\begin{aligned}\frac{d\Gamma}{dq^2}(B_s \rightarrow S\nu\bar{\nu}) &= \frac{AG_F^2 |V_{tq'} V_{tb}^*|^2 m_{B_s}^3 \alpha^2 |D_\nu(x_t)|^2}{2^8 \pi^5 \sin^4 \theta_W} \\ &\quad \times \phi^{3/2}(1, \hat{r}, \hat{s}) |f_+(q^2)|^2,\end{aligned}\quad (27)$$

where $A = \cos^2 \theta$ for $B_s \rightarrow f_0(980)$ transition and $A = 1$ for $B_s \rightarrow K_0^*(1430)$ decay. The functions $D_\nu(x_t)$ and $\phi(1, \hat{r}, \hat{s})$ are given as

$$D_\nu(x_t) = \frac{x_t}{8} \left(\frac{2 + x_t}{x_t - 1} + \frac{3x_t - 6}{(x_t - 1)^2} \ln x_t \right),$$

$$\phi(1, \hat{r}, \hat{s}) = 1 + \hat{r}^2 + \hat{s}^2 - 2\hat{r} - 2\hat{s} - 2\hat{r}\hat{s},$$

where

$$x_t = \frac{m_t^2}{m_W^2}, \quad \hat{r} = \frac{m_S^2}{m_{B_s}^2}, \quad \hat{s} = \frac{q^2}{m_{B_s}^2},$$

and

$$\begin{aligned}\frac{d\Gamma}{dq^2}(B_s \rightarrow Sl^+l^-) &= \frac{AG_F^2 |V_{tq'} V_{tb}^*|^2 m_{B_s}^3 \alpha^2}{3 \cdot 2^9 \pi^5} v \phi^{1/2}(1, \hat{r}, \hat{s}) \\ &\quad \times \left[\left(1 + \frac{2\hat{l}}{\hat{s}} \right) \phi(1, \hat{r}, \hat{s}) \alpha_1 + 12\hat{l}\beta_1 \right],\end{aligned}\quad (28)$$

where $\hat{l} = m_l^2/m_{B_s}^2$ and the expressions of α_1 and β_1 and v are given as

$$v = \sqrt{1 - \frac{4m_l^2}{q^2}},$$

$$\alpha_1 = \left| C_9^{\text{eff}} f_+(q^2) + \frac{2\hat{m}_b C_7^{\text{eff}} f_T(q^2)}{1 + \sqrt{\hat{r}}} \right|^2 + |C_{10} f_+(q^2)|^2,$$

$$\begin{aligned}\beta_1 &= |C_{10}|^2 \left[\left(1 + \hat{r} - \frac{\hat{s}}{2} \right) |f_+(q^2)|^2 \right. \\ &\quad \left. + (1 - \hat{r}) \text{Re}(f_+(q^2) f_-^*(q^2)) + \frac{1}{2} \hat{s} |f_-(q^2)|^2 \right],\end{aligned}$$

where $\hat{m}_b = m_b/m_{B_s}$.

IV. NUMERICAL ANALYSIS

This section encompasses our numerical analysis of the form factors $f_+(q^2)$, $f_-(q^2)$, $f_T(q^2)$, branching fractions, longitudinal lepton polarization asymmetries, and discussion. The sum rules expressions of the form factors depict that the main input parameters entering the expressions are Wilson coefficients C_7^{eff} , C_9^{eff} , and C_{10} ; elements of the CKM matrix V_{tb} , V_{ts} , and V_{td} ; leptonic decay constants f_{B_s} , $f_{K_0^*}$, and f_{f_0} ; Borel parameters M_1^2 and M_2^2 , as well as the continuum thresholds s_0 and s'_0 . The values for the quark and meson masses are given in Table I and other input values are presented in Table II.

TABLE I. Masses of quarks and mesons in MeV [24].

m_d	m_s	m_b	$m_{f_0(980)}$	$m_{K_0^*(1430)}$	m_{B_s}
3.5–6.0	104^{+26}_{-34}	4200^{+170}_{-70}	980 ± 10	1425 ± 50	5366.3 ± 0.6

TABLE II. Input values in numerical calculations [24–30].

Names	Values
C_7^{eff}	-0.313
C_9^{eff}	4.344
C_{10}	-4.669
$ V_{tb} $	$0.77^{+0.18}_{-0.24}$
$ V_{ts} $	$(40.6 \pm 2.7) \times 10^{-3}$
$ V_{td} $	$(7.4 \pm 0.8) \times 10^{-3}$
$f_{f_0(980)}(1 \text{ GeV})$	370 ± 20
$f_{K_0^*(1430)}(1 \text{ GeV})$	445 ± 50
f_{B_s}	209 ± 38
m_W	80.41 GeV
m_t	$(171.2 \pm 2.1) \text{ GeV}$

Note that the values of the decay constants of the $f_0(980)$ and $K_0^*(1430)$ mesons have been obtained from the QCD sum rules method at a fixed renormalization scale of 1 GeV [25].

The expressions for the form factors contain also four auxiliary parameters: Borel mass squares M_1^2 and M_2^2 and continuum threshold s_0 and s'_0 . These are not physical quantities, so the physical quantities, form factors, should be independent of them. The parameters s_0 and s'_0 , which are the continuum thresholds of the B_s and S mesons ($S = f_0(980), K_0^*(1430)$), respectively, are determined from the conditions that guarantee the sum rules to have the best stability in the allowed M_1^2 and M_2^2 region. The values of continuum thresholds calculated from the two-point QCD sum rules are taken to be $s_0 = 35 \text{ GeV}^2$ [31] and $s'_0 = (1.6 \pm 0.1) \text{ GeV}^2$ for $f_0(980)$ [30,32] and $s'_0 = (4.8 \pm 0.8) \text{ GeV}^2$ for $K_0^*(1430)$ [19]. The working regions for M_1^2 and M_2^2 are determined by requiring that not only the contributions of the higher states and continuum are effectively suppressed, but it guarantees that the contribu-

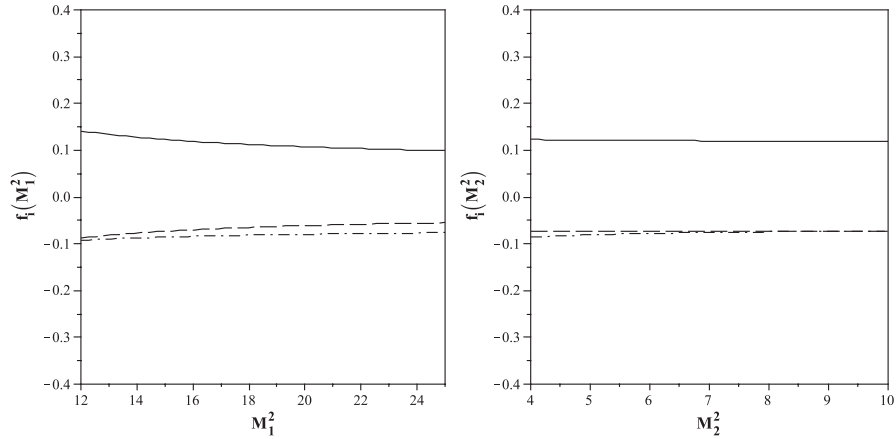


FIG. 3. The dependence of the form factors on M_1^2 and M_2^2 for $B_s \rightarrow f_0(980)$ decay. The solid line corresponds to f_+ , the dashed line f_- , and the dashed-dotted line f_T .

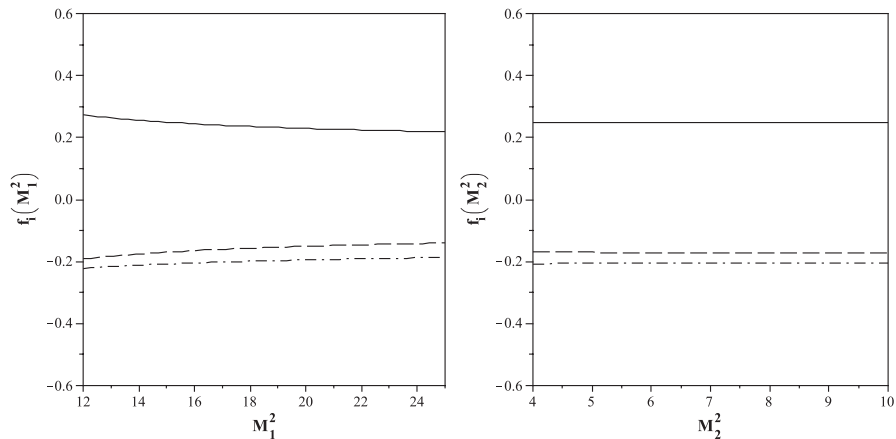


FIG. 4. The dependence of the form factors on M_1^2 and M_2^2 for $B_s \rightarrow K_0^*(1430)$ decay. The solid line corresponds to the f_+ , the dash line f_- and the dash dot line f_T .

TABLE III. The values of the form factors at $q^2 = 0$ for $M_1^2 = 18 \text{ GeV}^2$ and $M_2^2 = 7 \text{ GeV}^2$.

	$B_s \rightarrow f_0(980)$	$B_s \rightarrow K_0^*(1430)$
$f_+(0)$	0.12 ± 0.03	0.25 ± 0.05
$f_-(0)$	-0.07 ± 0.02	-0.17 ± 0.04
$f_T(0)$	-0.08 ± 0.02	-0.21 ± 0.04

TABLE IV. Parameters appearing in the form factors for $M_1^2 = 18 \text{ GeV}^2$, $M_2^2 = 7 \text{ GeV}^2$.

	$B_s \rightarrow f_0(980)$			$B_s \rightarrow K_0^*(1430)$		
	$f(0)$	α	β	$f(0)$	α	β
$f_+(q^2)$	0.12	1.05	-0.06	0.25	1.22	0.17
$f_-(q^2)$	-0.07	-1.25	0.78	-0.17	-1.60	0.16
$f_T(q^2)$	-0.08	-1.06	0.23	-0.21	-1.50	0.10

tions of higher dimensional operators are small. Both conditions are satisfied in the regions $12 \text{ GeV}^2 \leq M_1^2 \leq 25 \text{ GeV}^2$ and $4 \text{ GeV}^2 \leq M_2^2 \leq 10 \text{ GeV}^2$.

The dependence of the form factors f_+ , f_- , and f_T on M_1^2 and M_2^2 for $B_s \rightarrow f_0(980)l^+l^-/\nu\bar{\nu}$ are shown in Fig. 3, respectively. Figure 4 also depicts the dependence of the form factors on Borel mass parameters for $B_s \rightarrow K_0^*(1430)l^+l^-/\nu\bar{\nu}$.

These figures show a good stability of the form factors with respect to the Borel mass parameters in the working regions. Our numerical analysis shows that the contribution of the nonperturbative part is about 19% of the total and the main contribution comes from the perturbative part of the form factors.

The values of the form factors at $q^2 = 0$ are given in Table III.

In Ref. [10], the value of the $f_+^{B_s \rightarrow K_0^*(1430)}(0)$ has been previously calculated and is given as 0.24.

The sum rules for the form factors are truncated at about 7 GeV^2 and 5 GeV^2 below the perturbative cut for the $B_s \rightarrow f_0(980)$ and $B_s \rightarrow K_0^*(1430)$ decays, respectively, so to extend our results to the full physical region, we look for parametrization of the form factors in such a way that in the region $0 \leq q^2 \leq (m_{B_s} - m_S)^2$ this parametrization coincides with the sum rules prediction. Our numerical calculations show that the sufficient parametrization of the form factors with respect to q^2 is

$$f_i(q^2) = \frac{f_i(0)}{1 + \alpha\hat{q} + \beta\hat{q}^2}, \quad (29)$$

where $\hat{q} = q^2/m_{B_s}^2$. The values of the parameters $f_i(0)$, α , and β are given in the Table IV. The dependence of the form factors $f_+(q^2)$, $f_-(q^2)$, and $f_T(q^2)$ on q^2 are given in Figs. 5 and 6 for the $B_s \rightarrow f_0(980)$ and $B_s \rightarrow K_0^*(1430)$ decays, respectively. These figures also contain the form factors obtained via 3PSR [see Eqs. (22)–(24)]. The form factors and their fit functions coincide well in the interval $0 \leq q^2 \leq 11 \text{ GeV}^2$.

Now we would like to present the values of the branching ratios for the considered decays. Integrating Eqs. (27) and (28) over q^2 in the whole physical region and using the total mean life time $\tau_{B_s} = 1.466 \pm 0.059 \text{ ps}$ [24], the branching ratios of the $B_s \rightarrow f_0(980)l^+l^-/\nu\bar{\nu}$ and $B_s \rightarrow K_0^*(1430)l^+l^-/\nu\bar{\nu}$ are obtained. The differential decay branching ratios for the $B_s \rightarrow Sl^+l^-/\nu\bar{\nu}$ decays as functions of q^2 are shown in Figs. 7–12. Also the branching ratio values of these decays are obtained as presented in Table V, when only the short distance effects are considered. It should be remarked that our values for the branching ratios of the $B_s \rightarrow f_0(980)l^+l^-/\nu\bar{\nu}$ decays are related to $25^\circ \leq \theta \leq 55^\circ$.

Note that, the long distance (LD) effects for the charged lepton modes are not included in the values of Table V. With the LD effects, we introduce some cuts close to $q^2 = 0$ and around the resonances of J/ψ and ψ' and study the

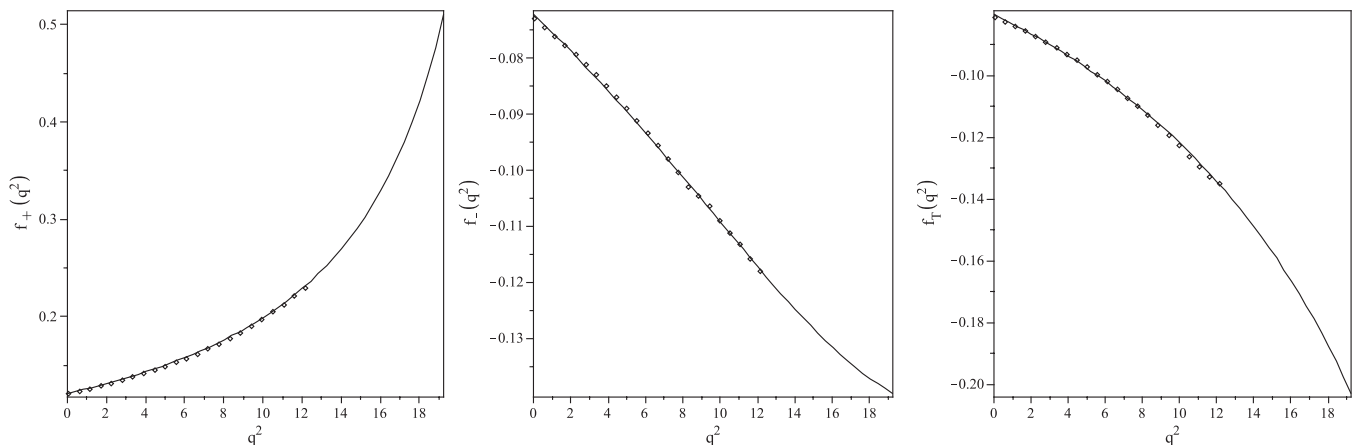


FIG. 5. The dependence of the form factors on q^2 at $M_1^2 = 18 \text{ GeV}^2$ and $M_2^2 = 7 \text{ GeV}^2$ for the $B_s \rightarrow f_0(980)$ transition. The small boxes correspond to the form factors, the solid lines belong to the fit parametrization of the form factors.

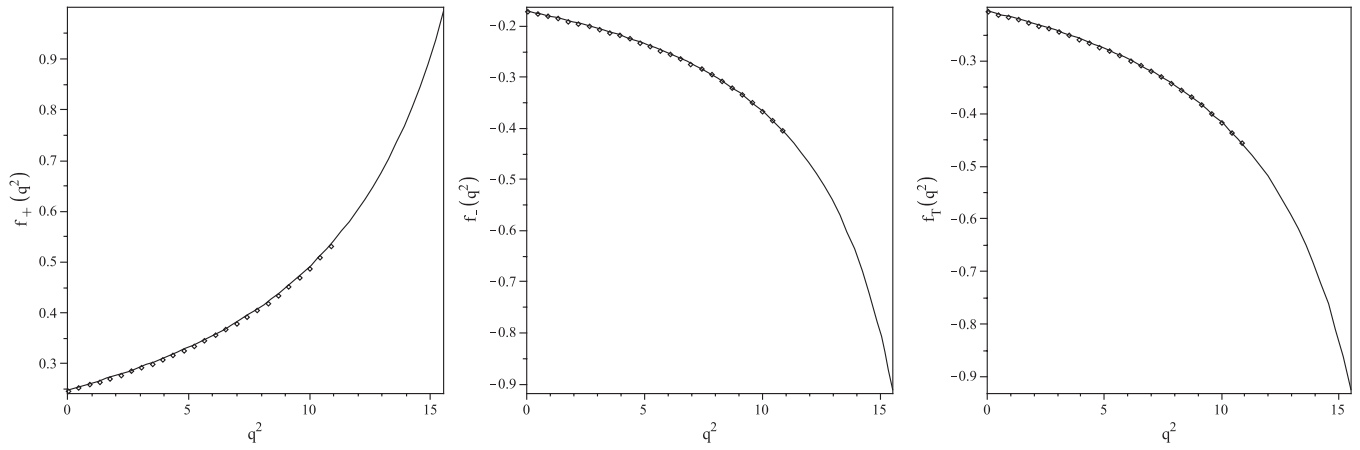


FIG. 6. The dependence of the form factors on q^2 at $M_1^2 = 18 \text{ GeV}^2$ and $M_2^2 = 7 \text{ GeV}^2$ for the $B_s \rightarrow K_0^*(1430)$ transition. The small boxes correspond to the form factors, the solid lines belong to the fit parametrization of the form factors.

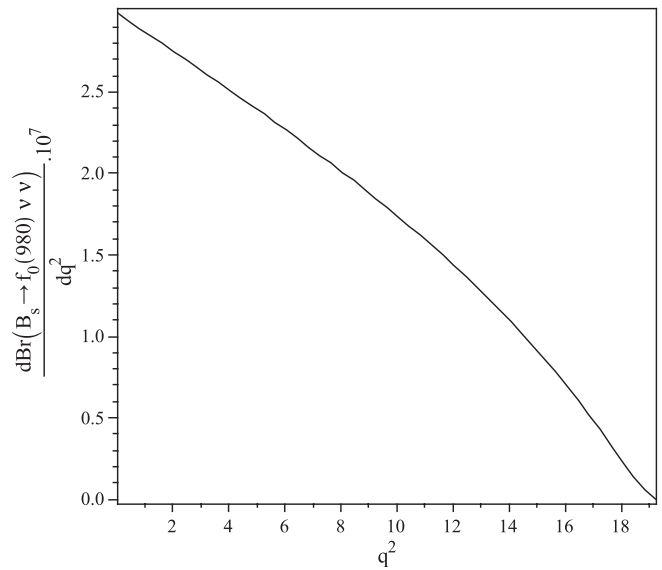
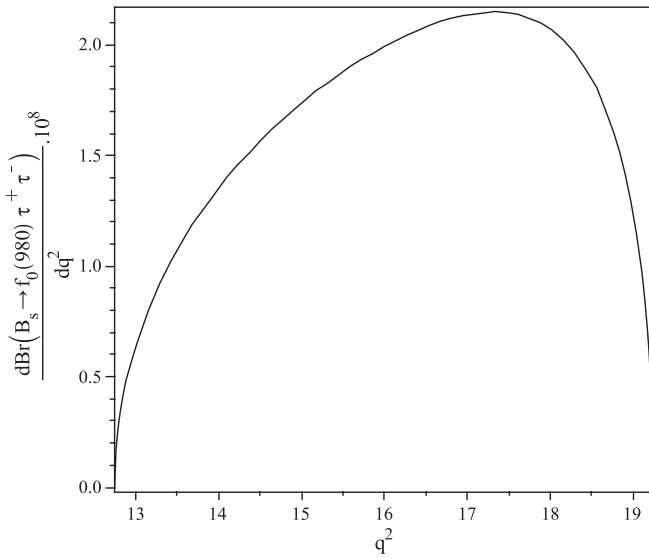


FIG. 7. The dependence of the differential decay branching fraction of the $B_s \rightarrow f_0(980)\tau^+\tau^-$ decay on q^2 .

FIG. 9. The same as Fig. 7 but for the $B_s \rightarrow f_0(980)\nu\bar{\nu}$.

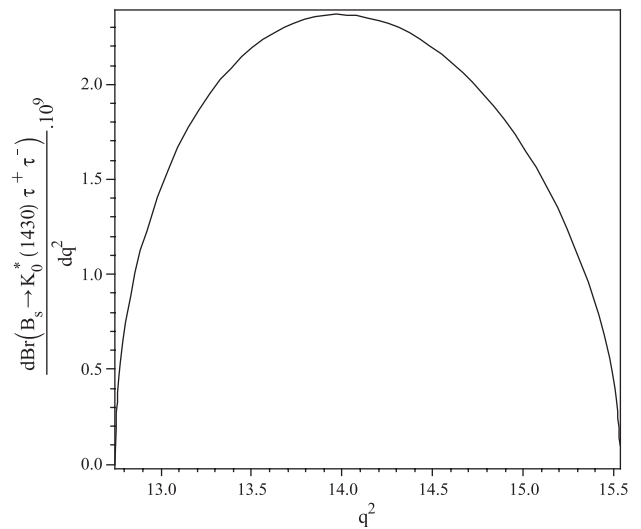
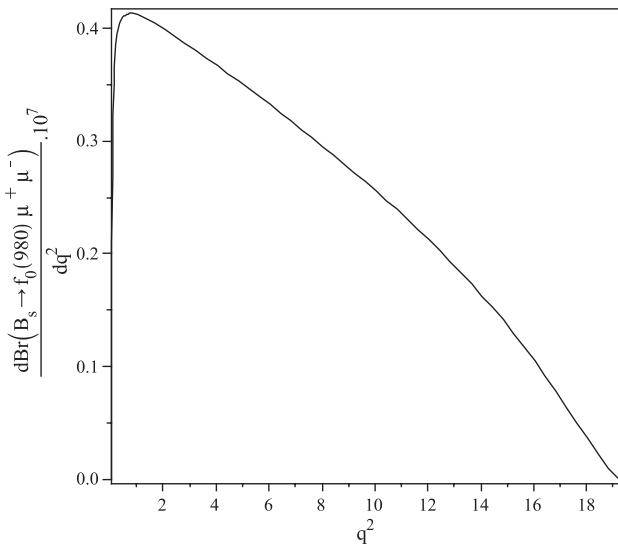
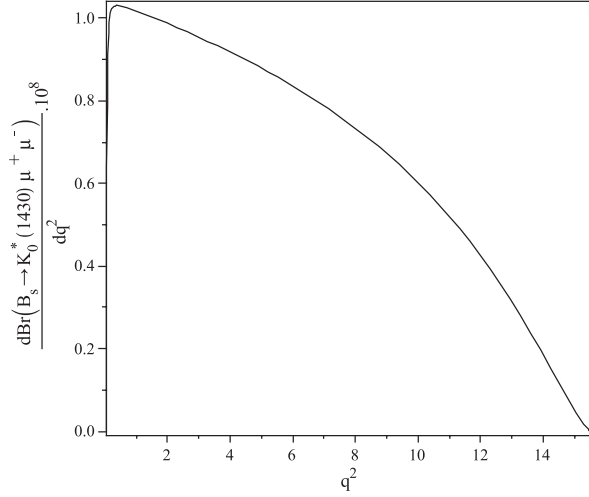
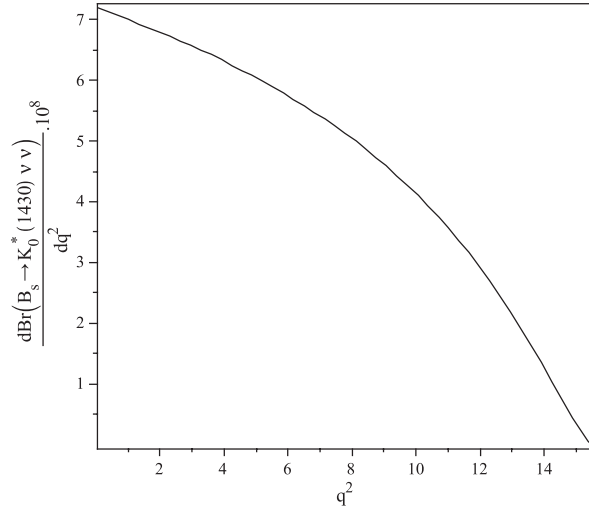


FIG. 8. The same as Fig. 7 but for the $B_s \rightarrow f_0(980)\mu^+\mu^-$.

FIG. 10. The dependence of the differential decay branching fraction of the $B_s \rightarrow K_0^*(1430)\tau^+\tau^-$ decay on q^2 .

FIG. 11. The same as Fig. 10 but for the $B_s \rightarrow K_0^*(1430)\mu^+\mu^-$.FIG. 12. The same as Fig. 10 but for the $B_s \rightarrow K_0^*(1430)\nu\bar{\nu}$.

three regions as follows:

$$\text{I: } \sqrt{q_{\min}^2} \leq \sqrt{q^2} \leq M_{J/\psi} - 0.20,$$

$$\text{II: } M_{J/\psi} + 0.04 \leq \sqrt{q^2} \leq M_{\psi'} - 0.10,$$

$$\text{III: } M_{\psi'} + 0.02 \leq \sqrt{q^2} \leq m_{B_c} - m_{D_{s1}}, \quad (30)$$

where $\sqrt{q_{\min}^2} = 2m_l$. In Table VI, we present the branching ratios in terms of the regions shown in Eq. (30).

The errors are estimated by the variation of the Borel parameters M_1^2 and M_2^2 , the variation of the continuum thresholds s_0 and s'_0 , the variation of b and s quark masses, and leptonic decay constants f_{B_s} , $f_{K_0^*}$, and f_{f_0} . The main uncertainty comes from the thresholds and the decay constants, which is about $\sim 18\%$ of the central value, while the other uncertainties are small, constituting a few percent.

Finally, we consider the longitudinal lepton polarization asymmetries for these decays. We have [23]

$$P_L = \frac{2\nu}{(1 + \frac{2\hat{l}}{s})\phi(1, \hat{r}, \hat{s})\alpha_1 + 12\hat{l}\beta_1} \text{Re} \left[\phi(1, \hat{r}, \hat{s}) \times \left(C_9^{\text{eff}} f_+(q^2) - \frac{2C_7 f_T(q^2)}{1 + \sqrt{\hat{r}}} \right) (C_{10} f_+(q^2))^* \right], \quad (31)$$

where ν , \hat{l} , \hat{r} , \hat{s} , $\phi(1, \hat{r}, \hat{s})$, α_1 , and β_1 were defined before. The dependence of the longitudinal lepton polarization asymmetries of the $B_s \rightarrow K_0^*(1430)$ and $B_s \rightarrow f_0(980)$ decays on the transferred momentum square q^2 are plotted in Figs. 13 and 14 in the region $0 \leq q^2 \leq (m_{B_s} - m_s)^2 \text{ GeV}^2$. Note that the results for the electron modes are similar to those for the muon modes.

TABLE V. Our values for the branching fractions of the mentioned decays by considering $M_1^2 = 18 \text{ GeV}^2$ and $M_2^2 = 7 \text{ GeV}^2$. The branching fraction values of the $B_s \rightarrow f_0(980)$ transitions correspond to $25^\circ \leq \theta \leq 55^\circ$.

Mods	Br	Mods	Br
$B_s \rightarrow f_0(980)\nu\bar{\nu}$	$(0.56-1.38) \times 10^{-7}$	$B_s \rightarrow K_0^*(1430)\nu\bar{\nu}$	$(2.48 \pm 0.62) \times 10^{-8}$
$B_s \rightarrow f_0(980)e^+e^-$	$(0.82-2.03) \times 10^{-8}$	$B_s \rightarrow K_0^*(1430)e^+e^-$	$(0.72 \pm 0.20) \times 10^{-8}$
$B_s \rightarrow f_0(980)\mu^+\mu^-$	$(0.81-2.02) \times 10^{-8}$	$B_s \rightarrow K_0^*(1430)\mu^+\mu^-$	$(0.71 \pm 0.20) \times 10^{-8}$
$B_s \rightarrow f_0(980)\tau^+\tau^-$	$(2.01-4.96) \times 10^{-9}$	$B_s \rightarrow K_0^*(1430)\tau^+\tau^-$	$(3.53 \pm 0.88) \times 10^{-10}$

TABLE VI. The branching ratios of the semileptonic $B_s \rightarrow K_0^*(1430)l^+l^-/\nu\bar{\nu}$ and $B_s \rightarrow f_0(980)l^+l^-/\nu\bar{\nu}$ decays including LD effects.

Mods	I	II	III
$Br(B_s \rightarrow f_0(980)e^+e^-)$	$(0.50-1.31) \times 10^{-8}$	$(1.38-3.39) \times 10^{-9}$	$(0.64-1.58) \times 10^{-9}$
$Br(B_s \rightarrow f_0(980)\mu^+\mu^-)$	$(0.49-1.29) \times 10^{-8}$	$(1.37-3.37) \times 10^{-9}$	$(0.63-1.57) \times 10^{-9}$
$Br(B_s \rightarrow f_0(980)\tau^+\tau^-)$	undefined	$(0.50-2.88) \times 10^{-9}$	$(1.68-4.12) \times 10^{-9}$
$Br(B_s \rightarrow K_0^*(1430)e^+e^-)$	$(0.52 \pm 0.13) \times 10^{-8}$	$(1.13 \pm 0.28) \times 10^{-9}$	$(0.51 \pm 0.13) \times 10^{-10}$
$Br(B_s \rightarrow K_0^*(1430)\mu^+\mu^-)$	$(0.52 \pm 0.13) \times 10^{-8}$	$(1.12 \pm 0.27) \times 10^{-9}$	$(0.50 \pm 0.12) \times 10^{-10}$
$Br(B_s \rightarrow K_0^*(1430)\tau^+\tau^-)$	undefined	$(0.79 \pm 0.20) \times 10^{-10}$	$(1.31 \pm 0.33) \times 10^{-10}$

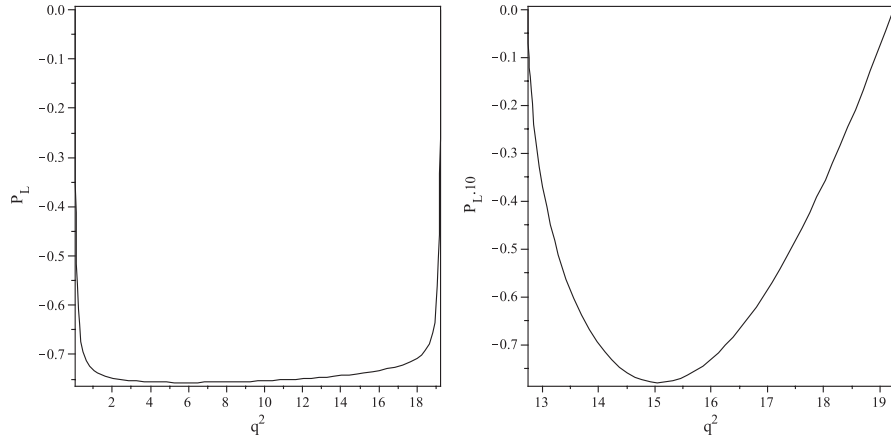


FIG. 13. Longitudinal lepton polarization asymmetry on q^2 . The left figure shows this quantity for the $B_s \rightarrow f_0(980)\mu^+\mu^-$ decay and the right belongs to the $B_s \rightarrow f_0(980)\tau^+\tau^-$.

Any experimental measurements on the branching fractions of these decays and those comparisons with the results of the phenomenological models like QCD sum rules could give valuable information about the nature of the $f_0(980)$ and $K_0^*(1430)$ mesons and strong interactions inside them.

In summary, we considered the $B_s \rightarrow f_0(980)l^+l^-/\nu\bar{\nu}$ and $B_s \rightarrow K_0^*(1430)l^+l^-/\nu\bar{\nu}$ channels and computed the relevant form factors considering the contributions of the quark condensate corrections. We also evaluated the total decay widths and the branching fractions of these decays. Finally, The dependence of the longitudinal lepton polarization asymmetries of the $B_s \rightarrow [f_0(980), K_0^*(1430)]$ decays on the transferred momentum square q^2 were plotted. Detection of these channels and their comparison with the

phenomenological models like QCD sum rules could give useful information about the structure of the $f_0(980)$ and $K_0^*(1430)$ scalar mesons.

ACKNOWLEDGMENTS

Partial support of the Shiraz University research council is appreciated. R. Khosravi would like to thank K. Azizi for his useful discussions.

APPENDIX

In this Appendix, the explicit expressions of the coefficients of the quark condensate entering the sum rules of the form factors $f_i(q^2)$, ($i = +, -, T$) are given.

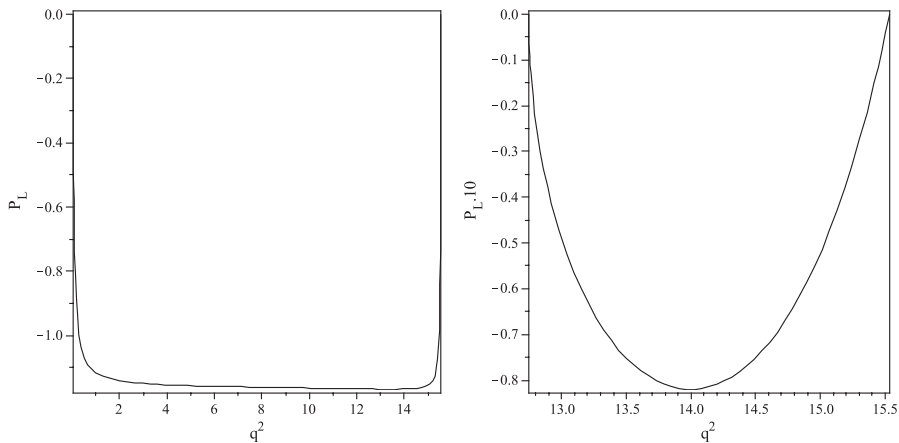


FIG. 14. Longitudinal lepton polarization asymmetry on q^2 . The left figure shows this quantity for the $B_s \rightarrow K_0^*(1430)\mu^+\mu^-$ decay and the right belongs to the $B_s \rightarrow K_0^*(1430)\tau^+\tau^-$.

$$\begin{aligned} \Pi_+^{\text{nonper}}(p^2, p'^2, q^2) = \langle s\bar{s} \rangle & \left\{ -\frac{1}{2} \frac{m_s}{rr'} + \frac{1}{3} \frac{m_0^2 m_{q'}}{rr'^2} - \frac{1}{6} \frac{m_0^2 m_b}{rr'^2} - \frac{1}{12} \frac{m_0^2 m_{q'}^3}{r^2 r'^2} + \frac{1}{12} \frac{m_0^2 m_b^3}{r^2 r'^2} + \frac{1}{6} \frac{m_0^2 m_{q'}}{r^2 r'} - \frac{1}{3} \frac{m_0^2 m_b}{r^2 r'} \right. \\ & + \frac{1}{4} \frac{m_s m_b^2}{r^2 r'} + \frac{1}{4} \frac{m_s m_{q'}^2}{rr'^2} - \frac{1}{2} \frac{m_b^3 m_s^2}{r^3 r'} + \frac{1}{4} \frac{m_0^2 m_b^3}{r^3 r'} + \frac{1}{4} \frac{m_{q'}^3 m_s^2}{r^2 r'^2} - \frac{1}{4} \frac{m_b^3 m_s^2}{r^2 r'^2} + \frac{1}{2} \frac{m_{q'}^3 m_s^2}{rr'^3} \\ & - \frac{1}{4} \frac{m_0^2 m_{q'}^3}{rr'^3} - \frac{1}{4} \frac{m_s m_b m_{q'}}{rr'^2} - \frac{1}{4} \frac{m_s m_b m_{q'}}{r^2 r'} - \frac{1}{6} \frac{m_0^2 m_b^2 m_{q'}}{r^2 r'^2} + \frac{1}{6} \frac{m_0^2 m_b m_{q'}^2}{r^2 r'^2} - \frac{1}{12} \frac{m_0^2 m_b q^2}{r^2 r'^2} \\ & + \frac{1}{12} \frac{m_0^2 m_{q'} q^2}{r^2 r'^2} - \frac{1}{2} \frac{m_b m_{q'}^2 m_s^2}{rr'^3} + \frac{1}{4} \frac{m_0^2 m_b m_{q'}^2}{rr'^3} + \frac{1}{4} \frac{m_b^2 m_{q'} m_s^2}{r^2 r'^2} - \frac{1}{4} \frac{m_b m_{q'}^2 m_s^2}{r^2 r'^2} + \frac{1}{4} \frac{m_b q^2 m_s^2}{r^2 r'^2} \\ & \left. - \frac{1}{4} \frac{m_{q'} q^2 m_s^2}{r^2 r'^2} + \frac{1}{2} \frac{m_b^2 m_{q'} m_s^2}{r^3 r'} - \frac{1}{4} \frac{m_0^2 m_b^2 m_{q'}}{r^3 r'} \right\}, \end{aligned}$$

$$\begin{aligned} \Pi_-^{\text{nonper}}(p^2, p'^2, q^2) = \langle s\bar{s} \rangle & \left\{ \frac{1}{6} \frac{m_0^2 m_b}{rr'^2} - \frac{1}{12} \frac{m_0^2 m_{q'}^3}{r^2 r'^2} - \frac{1}{12} \frac{m_0^2 m_b^3}{r^2 r'^2} + \frac{1}{6} \frac{m_0^2 m_{q'}}{r^2 r'} - \frac{1}{4} \frac{m_s m_b^2}{r^2 r'} + \frac{1}{4} \frac{m_s m_{q'}^2}{rr'^2} + \frac{1}{2} \frac{m_b^3 m_s^2}{r^3 r'} \right. \\ & - \frac{1}{4} \frac{m_0^2 m_b^3}{r^3 r'} + \frac{1}{4} \frac{m_{q'}^3 m_s^2}{r^2 r'^2} + \frac{1}{4} \frac{m_b^3 m_s^2}{r^2 r'^2} + \frac{1}{2} \frac{m_{q'}^3 m_s^2}{rr'^3} - \frac{1}{4} \frac{m_0^2 m_{q'}^3}{rr'^3} + \frac{1}{2} \frac{m_{q'} m_s^2}{rr'^2} + \frac{1}{2} \frac{m_b m_s^2}{r^2 r'} \\ & + \frac{1}{4} \frac{m_s m_b m_{q'}}{rr'^2} - \frac{1}{4} \frac{m_s m_b m_{q'}}{r^2 r'} + \frac{1}{12} \frac{m_0^2 m_b q^2}{r^2 r'^2} + \frac{1}{12} \frac{m_0^2 m_{q'} q^2}{r^2 r'^2} + \frac{1}{2} \frac{m_b m_{q'}^2 m_s^2}{rr'^3} - \frac{1}{4} \frac{m_b m_{q'}^2 m_0^2}{rr'^3} \\ & \left. + \frac{1}{4} \frac{m_b^2 m_{q'} m_s^2}{r^2 r'^2} + \frac{1}{4} \frac{m_b m_{q'}^2 m_s^2}{r^2 r'^2} - \frac{1}{4} \frac{m_b q^2 m_s^2}{r^2 r'^2} - \frac{1}{4} \frac{m_{q'} q^2 m_s^2}{r^2 r'^2} + \frac{1}{2} \frac{m_b^2 m_{q'} m_s^2}{r^3 r'} - \frac{1}{4} \frac{m_b^2 m_{q'} m_0^2}{r^3 r'} \right\}, \end{aligned}$$

$$\begin{aligned} \Pi_T^{\text{nonper}}(p^2, p'^2, q^2) = \langle s\bar{s} \rangle & \left\{ \frac{1}{2} \frac{m_s m_{q'}}{rr'} + \frac{1}{2} \frac{m_s m_b}{rr'} + \frac{1}{2} \frac{m_s m_b^3}{r^2 r'} + \frac{1}{2} \frac{m_s m_{q'}^3}{rr'^2} + \frac{1}{6} \frac{m_0^2 m_{q'}^2}{r^2 r'} + \frac{1}{6} \frac{m_0^2 m_b^4}{r^2 r'^2} - \frac{1}{6} \frac{m_0^2 m_{q'}^4}{r^2 r'^2} \right. \\ & - \frac{1}{6} \frac{m_0^2 m_b^2}{rr'^2} - \frac{1}{6} \frac{m_0^2 q^2}{rr'^2} + \frac{1}{6} \frac{m_0^2 q^2}{r^2 r'} - \frac{m_b^4 m_s^2}{r^3 r'} + \frac{1}{2} \frac{m_0^2 m_b^4}{r^3 r'} + \frac{1}{2} \frac{q^2 m_s^2}{rr'^2} + \frac{1}{2} \frac{m_{q'}^2 m_s^2}{rr'^2} - \frac{1}{2} \frac{m_b^2 m_s^2}{rr'^2} \\ & + \frac{1}{2} \frac{m_{q'}^4 m_s^2}{r^2 r'^2} - \frac{1}{2} \frac{m_b^4 m_s^2}{r^2 r'^2} + \frac{m_{q'}^4 m_s^2}{rr'^3} - \frac{1}{2} \frac{m_0^2 m_{q'}^4}{rr'^3} - \frac{1}{2} \frac{m_b^2 m_s^2}{r^2 r'} + \frac{1}{2} \frac{m_{q'}^2 m_s^2}{r^2 r'} - \frac{1}{2} \frac{q^2 m_s^2}{r^2 r'} \\ & - \frac{1}{2} \frac{m_s m_b^2 m_{q'}}{rr'^2} - \frac{1}{2} \frac{m_s m_b m_{q'}^2}{r^2 r'} + \frac{1}{4} \frac{m_0^2}{rr'} - \frac{1}{6} \frac{m_0^2 m_b^2 q^2}{r^2 r'^2} + \frac{1}{6} \frac{m_0^2 m_{q'}^2 q^2}{r^2 r'^2} - \frac{1}{6} \frac{m_0^2 m_b m_{q'}}{rr'^2} \\ & + \frac{1}{6} \frac{m_0^2 m_b m_{q'}}{r^2 r'} - \frac{m_b^2 m_{q'}^2 m_s^2}{rr'^3} + \frac{1}{2} \frac{m_b^2 m_{q'}^2 m_0^2}{rr'^3} + \frac{1}{2} \frac{m_b^2 q^2 m_s^2}{r^2 r'^2} - \frac{1}{2} \frac{m_{q'}^2 q^2 m_s^2}{r^2 r'^2} + \frac{m_b^2 m_{q'}^2 m_s^2}{r^3 r'} \\ & \left. - \frac{1}{2} \frac{m_b^2 m_{q'}^2 m_0^2}{r^3 r'} \right\}, \end{aligned}$$

where $r = p^2 - m_b^2$, $r' = p'^2 - m_{q'}^2$, $m_0^2 = 0.8 \pm 0.2 \text{ GeV}^2$, $\langle s\bar{s} \rangle = (0.8 \pm 0.2) \langle u\bar{u} \rangle$, and $\langle u\bar{u} \rangle = -(0.240 \pm 0.010 \text{ GeV})^3$ that we choose the value of the condensates at a fixed renormalization scale of about 1 GeV.

-
- [1] R. L. Jaffe, Phys. Rev. D **15**, 267 (1977).
[2] M. N. Achasov *et al.*, Phys. Lett. B **438**, 441 (1998).
[3] N. N. Achasov and V. V. Gubin, Phys. Rev. D **56**, 4084 (1997).
[4] J. Weinstein and N. Isgur, Phys. Rev. Lett. **48**, 659 (1982); Phys. Rev. D **27**, 588 (1983).
[5] G. Janssen, B. C. Pearce, K. Holinde, and J. Speth, Phys. Rev. D **52**, 2690 (1995).
[6] R. Kaminski, L. Lesniak, and J. P. Maillet, Phys. Rev. D **50**, 3145 (1994); R. Kaminski, L. Lesniak, and B. Loiseau, Phys. Lett. B **413**, 130 (1997).
[7] J. A. Oller and E. Oset, Nucl. Phys. **A620**, 438 (1997).
[8] M. P. Locher, V. E. Markushin, and H. Q. Zheng, Eur. Phys. J. C **4**, 317 (1998).
[9] M. Z. Yang, Mod. Phys. Lett. A **21**, 1625 (2006).
[10] M. Z. Yang, Phys. Rev. D **73**, 034027 (2006).
[11] N. A. Tornqvist, Phys. Rev. Lett. **49**, 624 (1982).
[12] N. A. Tornqvist, Z. Phys. C **68**, 647 (1995).

- [13] E. van Beveren, G. Rupp, and M. D. Scadron, *Phys. Lett. B* **495**, 300 (2000).
- [14] F.E. Close, N. Isgur, and S. Kumano, *Nucl. Phys.* **B389**, 513 (1993).
- [15] E. M. Aitala *et al.* (E791 Collaboration), *Phys. Rev. Lett.* **86**, 765 (2001).
- [16] H. Y. Cheng, *Phys. Rev. D* **67**, 034024 (2003); W. Wang, Y.L. Shen, Y. Li, and C. D. Lu, *Phys. Rev. D* **74**, 114010 (2006).
- [17] I. Bediaga, F. S. Navarra, and M. Nielsen, *Phys. Lett. B* **579**, 59 (2004).
- [18] V. V. Anisovich, L. G. Dakhno, and V. A. Nikonov, *Yad. Fiz.* **67**, 1593 (2004) [*Phys. At. Nucl.* **67**, 1571 (2004)].
- [19] D. S. Du, J. W. Li, and M. Z. Yang, *Phys. Lett. B* **619**, 105 (2005).
- [20] P. Colangelo, F. De Fazio, P. Santorelli, and E. Scrimieri, *Phys. Rev. D* **53**, 3672 (1996).
- [21] T.M. Aliev, K. Azizi, and M. Savci, *Phys. Rev. D* **76**, 074017 (2007).
- [22] N. G. Deshpande, J. Trampetic, and K. Panose, *Phys. Rev. D* **39**, 1461 (1989); C. S. Lim, T. Morozumi, and A. I. Sanda, *Phys. Lett. B* **218**, 343 (1989).
- [23] C.H. Chen, C. Q. Geng, C. C. Lih, and C. C. Liu, *Phys. Rev. D* **75**, 074010 (2007).
- [24] C. Amsler *et al.* (Particle Data Group), *Phys. Lett. B* **667**, 1 (2008).
- [25] H. Y. Cheng, C. K. Chua, and K. C. Yang, *Phys. Rev. D* **73**, 014017 (2006).
- [26] A. J. Buras and M. Muenz, *Phys. Rev. D* **52**, 186 (1995).
- [27] V. Bashiry and K. Azizi, *J. High Energy Phys.* **07** (2007) 064.
- [28] A. Ceccucci, Z. Ligeti, and Y. Sakai (Particle Data Group), *J. Phys. G* **33**, 139 (2006).
- [29] A. Faessler *et al.*, *Eur. Phys. J. direct C* **4**, 1 (2002).
- [30] P. Colangelo and A. Khodjamirian, in *At the Frontier of Particle Physics/Handbook of QCD*, edited by M. Shifman (Word Scientific, Singapore, 2001), Vol. 3, p. 1495.
- [31] M. A. Shifman, A. I. Vainshtein, and V. I. Zakharov, *Nucl. Phys.* **B147**, 385 (1979).
- [32] I. Bediaga and M. Nielsen, *Phys. Rev. D* **68**, 036001 (2003).